

# Spontaneous crystallization and filamentation of solitons in dipolar condensates

Kazimierz Lakomy,<sup>1</sup> Rejish Nath,<sup>2</sup> and Luis Santos<sup>1</sup>

<sup>1</sup>*Institut für Theoretische Physik, Leibniz Universität, Hannover, Appelstrasse 2, D-30167, Hannover, Germany*

<sup>2</sup>*Max Planck Institute for the Physics of Complex Systems, Nöthnitzer Strasse 38, D-01187 Dresden, Germany*

(Dated: June 16, 2022)

Inter-site interactions play a crucial role in polar gases in optical lattices even in the absence of hopping. We show that due to these long-range interactions a destabilized stack of quasi-one dimensional Bose-Einstein condensates develops a correlated modulational instability in the non-overlapping sites. Interestingly, this density pattern may evolve spontaneously into soliton filaments or a crystal of solitons that can be so created for the first time in ultra-cold gases. These self-assembled structures may be observed under realistic conditions within current experimental feasibilities.

PACS numbers: 03.75.Lm, 03.75.Kk, 05.30.Jp

Recent experiments are opening new avenues for the study of the fascinating physics of dipolar gases [1, 2]. These gases present a significant electric or magnetic dipole-dipole interactions, which being long-range and anisotropic differ significantly from the short-range isotropic interactions usually dominant in quantum gases. Ultra-cold polar gases in optical lattices are particularly interesting. Contrary to the non-dipolar case, polar lattice gases are characterized by significant non-local inter-site interactions that result in a rich variety of novel physical phenomena [2, 3]. Remarkably, the inter-site interactions play a crucial role even in deep lattices where hopping is negligible. In particular, dipolar Bose-Einstein condensates (BECs) in non-overlapping lattice sites share common excitations modes. This collective character enhances roton-like features in the excitation spectrum [4] and modifies the BEC stability, as recently shown experimentally [5].

Quasi-1D geometries allow for the existence of BEC solitons and hence modulational instability in these systems leads to the formation of 1D patterns, so-called soliton trains [6]. On the contrary, dynamical instability in higher-dimensional BECs is typically followed by condensate collapse [7]. In consequence, solitons patterns in higher dimensions, as e.g. 2D crystals of solitons, are fundamentally prevented in non-polar BECs.

In this Letter we show that the destabilization of a dipolar BEC confined in a stack of non-overlapping quasi-1D tubes may be followed by the spontaneous self-assembly of stable soliton filaments or a 2D crystal of solitons, providing a route for the first realization of self-sustained 2D arrangements of BEC solitons. This dynamical self-assembly stems from the correlated character of the corresponding modulational instability. While for non-dipolar condensates the instability in each lattice site would develop independently, the non-local dipolar interactions couple the non-overlapping BECs to form a density pattern shared by all sites. As we show, corre-

lated modulational instability may be observable in current Chromium experiments.

The dynamically formed soliton filaments resemble dipolar chains of classical dipoles [8], as well as chains predicted for polar molecules [9, 10]. However, compared to the latter, soliton filamentation is expected to occur for smaller dipole moments due to the many-body character of each soliton. Remarkably, inverting the sign of the dipolar interactions results in the development of an anti-correlated density pattern followed by the spontaneous formation of a stable crystal of solitons. This 2D soliton crystal resembles the Wigner-like crystal predicted for polar molecules [11, 12]. However, contrary to the latter, it is dynamically formed and self-maintained by a non-trivial interplay between intra-tube attractive and inter-tube repulsive dipolar interactions.

We study below a dipolar BEC confined in a stack of quasi-1D tubes formed by an optical lattice (Fig. 1). The lattice is assumed to be sufficiently deep to suppress inter-site hopping. In each of the  $N_m$  lattice sites the  $xy$ -confinement is approximated by a harmonic potential with frequency  $\omega_{\perp}$ , whereas for simplicity we assume no confinement along  $z$  direction. We consider atoms

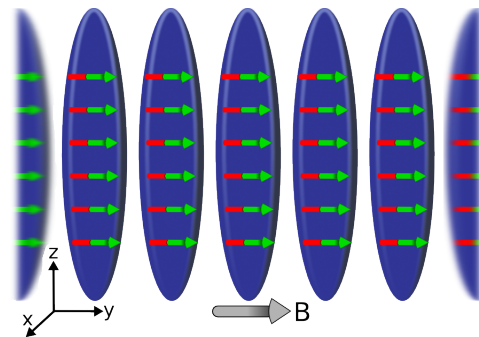


FIG. 1. (Color online) Scheme of the stack of disjoint quasi-1D dipolar BECs.

with a magnetic dipole moment  $\mu$  (the results are equally valid for electric dipoles, as e.g. polar molecules) oriented along  $y$  direction by an external magnetic field. The dipoles interact with each other via the dipole-dipole potential  $V_d(\mathbf{r} - \mathbf{r}') = g_d (1 - 3 \cos^2 \theta) / |\mathbf{r} - \mathbf{r}'|^3$ , where  $g_d = \mu_0 \mu^2 / 4\pi$ , with  $\mu_0$  being the vacuum permeability and  $\theta$  the angle formed by the vector joining the two interacting particles and the dipole moment direction.

We assume the chemical potential much smaller than  $\hbar\omega_\perp$  (this assumption is self-consistently verified in our calculations). Hence, we can factorize the BEC wave function at each site  $j$ ,  $\Psi_j(\mathbf{r}) = \phi_j(x, y) \psi_j(z)$ , with  $\phi_j(x, y)$  the ground-state wave function of the  $xy$  harmonic oscillator. Treating the dipolar potential in the Fourier space [13] we arrive at a system of  $N_m$  coupled 1D Gross-Pitaevskii equations describing the BEC stack:

$$i\hbar\partial_t \psi_j(z) = \left[ -\frac{\hbar^2}{2m} \partial_z^2 + \frac{g}{2\pi l_\perp^2} |\psi_j(z)|^2 + \frac{g_d}{3} \sum_{m=0}^{N_m-1} \int \frac{dk_z}{2\pi} e^{ik_z z} \hat{n}_m(k_z) F_{mj}(k_z) \right] \psi_j(z), \quad (1)$$

where  $\hat{n}_m(k_z)$  is the Fourier transform of the axial density  $n_m(z)$  at site  $m$ ,

$$F_{mj}(k_z) \equiv \int \frac{dk_x dk_y}{\pi} \left( \frac{3k_y^2}{k_x^2 + k_y^2 + k_z^2} - 1 \right) \times e^{-\frac{1}{2}(k_x^2 + k_y^2)l_\perp^2 - ik_y(m-j)\Delta}, \quad (2)$$

$l_\perp = \sqrt{\hbar/m\omega_\perp}$  is the  $xy$  oscillator length,  $\Delta$  is the lattice spacing, and  $g = 4\pi a \hbar^2/m$ .

Starting from a homogeneous on-site linear density  $n_0$  we are interested in the dynamics that follows the destabilization of the condensate after an abrupt change of the scattering length  $a$ . A substantial insight into the first stages of the post-instability dynamics is provided by the analysis of the elementary excitations of the condensate.

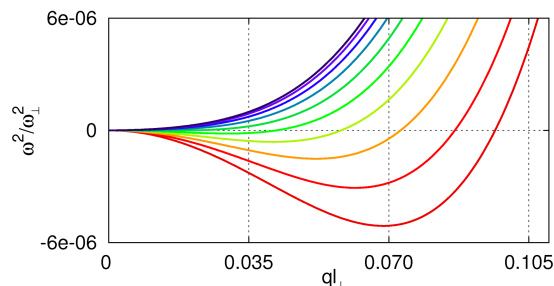


FIG. 2. (Color online) Bogoliubov spectrum for a Chromium BEC with a density  $10^{14} \text{ cm}^{-3}$  and  $a = -8.5a_0$  ( $a_0$  is the Bohr radius), occupying  $N_m = 10$  sites of a lattice with the inter-site spacing  $\Delta = 512 \text{ nm}$  and a lattice depth of  $13.3E_R$  (recoil energy), which results in the  $\omega_\perp = 2\pi \cdot 26.7 \text{ kHz}$ , and  $l_\perp = 85.3 \text{ nm}$ . Here,  $q_c = 0.07/l_\perp$ .

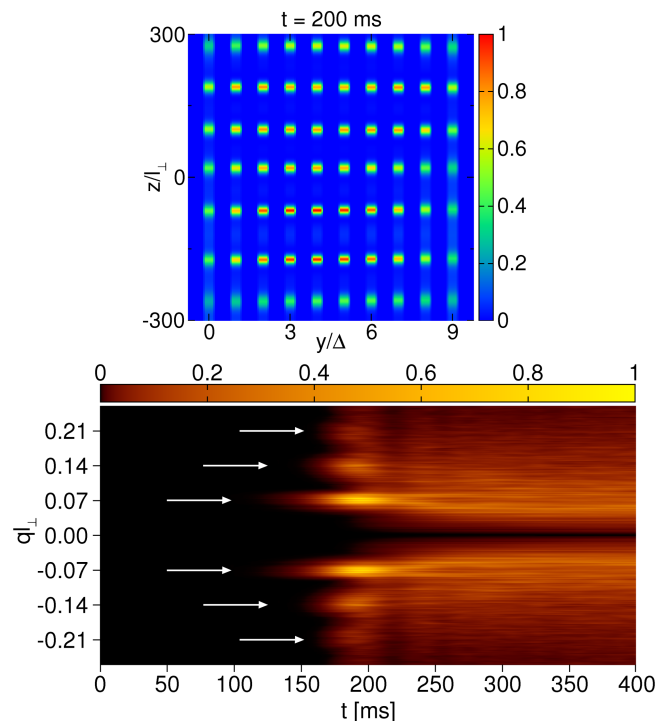


FIG. 3. (Color online) (top) BEC wave function's density plot after 200 ms of the time evolution for the same parameters as in Fig. 2. For plotting purposes the  $y$ -width of the tubes has been magnified. (bottom) Dynamics of the Fourier transform of the associated column density  $\Sigma(z, t)$ . The dominating  $q = 0$  peak has been removed for clarity and the remaining distribution has been normalized to the maximum. The arrows indicate the harmonics of  $q_c$ .

To this end we introduce a perturbation of the homogeneous solution,  $\psi_j(z, t) = [\sqrt{n_0} + \chi_j(z, t)] e^{-i\mu_j t/\hbar}$ , with  $\chi_j(z, t) = u_j e^{i(zq - \omega t)} + v_j^* e^{-i(zq - \omega t)}$ , where  $\mu_j$  is the chemical potential in a site  $j$ , and  $q$  and  $\omega$  are the  $z$ -momentum and the frequency of the elementary excitations, respectively. Employing this ansatz in Eq.(1) we arrive at the corresponding Bogoliubov-de Gennes equations yielding the excitation spectrum and the Bogoliubov coefficients  $u_j$  and  $v_j$ . Interestingly, even in absence of hopping, dipolar inter-site interactions result in a collective character of the excitations that are shared among all sites. In consequence, the excitation spectrum acquires a band-like character [4] as depicted in Fig. 2.

Modes with imaginary frequency are associated with dynamical instability. For non-dipolar gases, inter-site interactions are negligible and hence all transversal modes remain degenerated. As a result, modulational instability develops independently in each site and no correlated density pattern occurs during the post-instability dynamics. The situation dramatically changes for sufficiently large dipole moment, as the inter-site interactions lift the degeneracy between transversal modes. In particular, the most unstable mode becomes significantly more

unstable than other modes, as shown in Fig. 2, governing the BEC dynamics within the linear regime. Crucially, this most unstable mode is not only characterized by a  $z$ -momentum  $q_c$  (associated with the minimum of  $\omega^2$  in Fig. 2) setting the modulational instability in each wire, but also by a transversal dependence along the  $y$  direction locking the density pattern between sites. As a result, during the first stages of the post-instability dynamics a correlated modulational instability develops. Interestingly, our numerical simulations predict that this phenomenon may be observed in existing Chromium experiments.

Fig. 3 (top) depicts the case of a Chromium BEC destabilized by an abrupt change of  $a > 0$  into a sufficient  $a < 0$  by means of a Feshbach resonance. The numerical solution of Eq. (1) shows that a correlated density pattern develops, in spite of the absence of inter-site hopping. As shown in Fig. 3 (top) this instability pattern survives well into the non-linear regime where the density modulation cannot be considered any more as a perturbation of the original homogeneous on-site BECs. In typical experiments the density alignments may be more easily monitored investigating the column density  $\Sigma(z) \equiv \sum_m n_m(z)$ . Contrary to the uncorrelated case, for which  $\Sigma(z)$  would show no clear structure, the correlated instability results in periodically modulated  $\Sigma(z)$ . Fig. 3 (bottom) shows the dynamics of the Fourier transform of  $\Sigma(z, t)$  that is clearly characterized by the appearance of harmonics of  $q_c$  (compare Fig. 2 and Fig. 3 (bottom)).

The density modulation evolves into a correlated pattern of solitons, as seen in Fig. 3 (top). Solitons are created in an excited state, with both internal breathing excitation and center-of-mass motion. As a result, for small dipolar interactions the correlated density modulation is destroyed during the subsequent non-linear evolution and the positions of solitons at different sites become uncorrelated, not differing qualitatively from the case of non-polar gases. Sufficiently large inter-site interactions crucially change this picture, since correlated solitons at neighboring sites experience an attractive inter-site potential. The effective binding energy for a soliton dimer acquires the form

$$E_b = (-2g_d/\Delta^3)G(\delta/\Delta) \quad (3)$$

where we have approximated the solitons by Gaussians of width  $\delta$ , such that  $l_\perp \ll \delta, \Delta$ . Note that the binding energy between solitons differs from that of point-like distributions  $(-2g_d/\Delta^3)$  by the regularization function

$$G(x) \simeq \frac{e^{1/4x^2}}{4\sqrt{2\pi}x^3} \left[ (x^2+1)K_0\left(\frac{1}{4x^2}\right) + (x^2-1)K_1\left(\frac{1}{4x^2}\right) \right] \quad (4)$$

with  $K_n$  the modified Bessel function of second kind. As a result of this inter-site soliton attraction, and although the initial periodicity of the modulation (as that

of Fig. 3 (top)) is in general lost, self-assembled soliton filaments form spontaneously (Fig. 4) when the center-of-mass kinetic energy of the solitons acquired in the post-instability dynamics cannot overcome the binding energy given by Eq. (3). This occurs for a sufficiently large value of the dipole moment that depends non-trivially on  $g$  and the initial density  $n_0$ .

Fig. 4 shows our results for three distinct filamentation regimes governed by a value of the dipole moment  $\mu$ . In order to compare these different cases for the same initial configuration we choose for each value of  $\mu$  the appropriate value of  $a$  that results in the same value of  $q_c$  and so in the same initial number of solitons in all of the cases. For the parameters considered, no filamentation is observed for  $\mu = \mu_{Cr}$  (Chromium dipole moment). On the contrary, the case of  $1.5\mu_{Cr}$  already shows the formation of a gas of filaments that can be easily tracked from an analysis of the time evolution of the system. These filaments of different lengths present a highly non-trivial dynamics, including filament-filament interactions, string-like excitations, soliton breathing, and filament center-of-mass motion (although their mobility is handicapped by

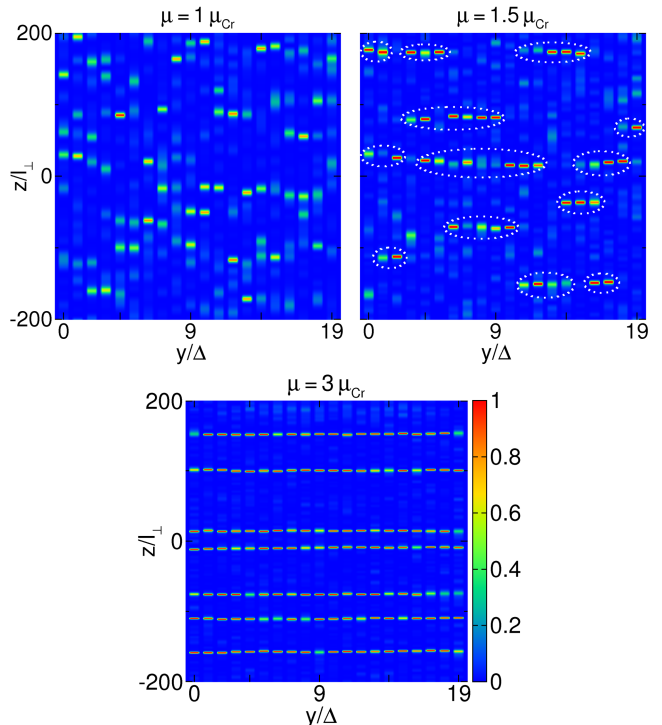


FIG. 4. (Color online) BEC density distribution after 500 ms of the time evolution in  $N_m=20$  lattice sites for  $\mu = \mu_{Cr}$  (top left),  $\mu = 1.5\mu_{Cr}$  (top right) and  $\mu = 3.0\mu_{Cr}$  (bottom) with  $a = -16.1a_0$ ,  $a = -20.1a_0$  and  $a = -41.7a_0$ , respectively (see text). The remaining parameters are chosen as in the case of Fig. 2. Ellipses in the top right figure indicate filaments trackable in the dynamics. For comparison purposes, we use the maximum density in the top-left figure as the saturation threshold for all density plots.

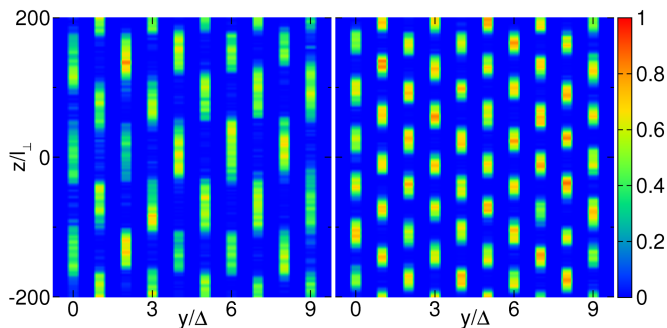


FIG. 5. (Color online) Spontaneous crystallization of solitons in the case of negative  $g_d$ . Here,  $a = 306a_0$ ,  $\mu = 6\mu_{Cr}$  and the other parameters as in Fig. 2. (left) Density plot after 2500 ms without ramping of  $a$ . (right) Density plot after 200 ms applying the ramping of  $a$  with  $a^i = 306a_0$ ,  $a^f = 275a_0$ ,  $t_0 = 50$  ms,  $r = 0.0095$  (see [14]). We normalize the density plot to the maximum value of the right panel.

their enlarged effective mass). Ultimately, for  $\mu = 3\mu_{Cr}$  strongly bound filaments of the maximum possible length  $N_m$  form spontaneously.

Interestingly, the sign of  $g_d$  may be inverted by means of transversal magnetic fields [15] or microwave dressing in the case of polar molecules [16]. Note that, although we consider this case for its theoretical simplicity, qualitatively the same results may be obtained orienting the dipoles along the tubes. In both of these cases, the most-unstable Bogoliubov mode presents a staggered  $y$ -dependence that results in an anti-correlated density pattern with maxima in a given site aligned with minima in the neighboring ones. Strikingly, for a sufficiently strong dipole moment, this structure acts as a seed for the dynamical formation of a permanent 2D crystal of solitons as shown in Fig. 5.

While purely repulsive interactions sustain the 2D Wigner-like crystals proposed for polar molecules [11, 12], the crystal of solitons is self-maintained by a subtle interplay of dipolar inter-tube repulsion and intra-tube attraction. Due to the anti-correlated character of the density modulation, solitons in neighboring sites provide an effective potential barrier that prevents mutually attracting solitons in the same tube to come together, hence keeping the crystal stable.

Typically, however, this repulsive barrier is initially insufficient to prevent solitons from merging. As a result the initial number of solitons decreases. This process ceases when the effective barriers maintain the solitons at an equilibrium distance and the soliton crystal settles. The equilibration time may be shortened by a smooth ramping of  $a$  down, starting when the soliton number predicted by the Bogoliubov analysis is reached [14]. As a result of the ramping, the width of the solitons is reduced, which in turn makes the potential barriers more effective, allowing the crystal to reach its final form faster.

Finally, we note that polar molecules, as KRb [17], pos-

sess typically dipole moments larger than 0.5 Debye, i.e. an effective  $\mu > 5\mu_{Cr}$ . Large dipole values may be also attained in atomic species. In particular, Dysprosium possesses a dipole moment  $\mu = 1.7\mu_{Cr}$  [18]. Hence, dynamical filamentation and crystallization should be observable in those systems under realistic experimental conditions.

In conclusion, the dipolar inter-site interactions in a destabilized dipolar BEC confined in a stack of quasi-1D tubes induce an interesting dynamics characterized by the development of a correlated modulational instability in the non-overlapping sites. For a sufficiently large dipole moment this density modulation seeds the spontaneous self-assembly of soliton filaments or a soliton crystal, depending on the sign of the dipolar interactions. Contrary to filaments and crystals of individual molecules, filaments and crystals of solitons self-assemble spontaneously just by simply destabilizing the condensate. Moreover, we expect that due to the many-body character of the constituent solitons the dipole moment necessary for observing these structures may be significantly reduced and that they may be attainable with partially polarized polar molecules or highly magnetic atoms, paving a promising route towards the first realization of 2D patterns of solitons in ultra-cold gases and, to the best of our knowledge, in nonlinear optics as well.

We acknowledge the support of the Center of Excellence QUEST and the German-Israeli Foundation.

- 
- [1] M. Baranov, *Physics Reports* **464**, 71 (2008).
  - [2] T. Lahaye *et al.*, *Reports on Progress in Physics* **72**, 126401 (2009).
  - [3] C. Trefzger *et al.*, [arXiv:1103.3145](https://arxiv.org/abs/1103.3145).
  - [4] M. Klawunn and L. Santos, *Phys. Rev. A* **80**, 013611 (2009).
  - [5] S. Müller *et al.*, [arXiv:1105.5015](https://arxiv.org/abs/1105.5015).
  - [6] K. E. Strecker *et al.*, *Nature* **417**, 150 (2002).
  - [7] E. A. Donley *et al.*, *Nature* **412**, 295 (2001).
  - [8] P. I. C. Teixeira, J. M. Tavares, and M. M. Telo da Gama, *J. Phys. Cond. Matt.* **12**, R411 (2000).
  - [9] D.-W. Wang, M. D. Lukin, and E. Demler, *Phys. Rev. Lett.* **97**, 180413 (2006).
  - [10] M. Klawunn, J. Duhme, and L. Santos, *Phys. Rev. A* **81**, 013604 (2010).
  - [11] H. P. Büchler *et al.*, *Phys. Rev. Lett.* **98**, 060404 (2007).
  - [12] G. Pupillo *et al.*, *Phys. Rev. Lett.* **100**, 050402 (2008).
  - [13] K. Góral and L. Santos, *Phys. Rev. A* **66**, 023613 (2002).
  - [14] The ramping we employ is of the form  $a(t) = a^i\theta(-t + t_0) + \theta(t - t_0)(a^f + (a^i - a^f)\exp(-r^2(t - t_0)^2))$ , with  $\theta$  the Heaviside function,  $t_0$  the ramping initialization time,  $a^i$  and  $a^f$  the initial and final scattering length, respectively, and  $r$  the ramping rate.
  - [15] S. Giovanazzi, A. Görlitz, and T. Pfau, *Phys. Rev. Lett.* **89**, 130401 (2002).
  - [16] A. Micheli *et al.*, *Phys. Rev. A* **76**, 043604 (2007).
  - [17] K.-K. Ni *et al.*, *Nature* **464**, 1324 (2010).
  - [18] M. Lu, S. H. Youn, and B. L. Lev, *Phys. Rev. A* **83**, 012510 (2011).